

BROADBAND DIELECTRIC WAVEGUIDE COUPLER AND SIX-PORT NETWORK

Feng Zheng-he

Department of Radio and Electronics
Tsing-hua University, Beijing, China

Abstract

A new structure of dielectric waveguide coupler and power divider has been described which has merits such as simple construction, flat frequency response, good repeatability and stability. The theoretical and measurement data are given in the paper. The six-port network in which the same technique is used has been developed. The design and performance data are also presented.

Directional Coupler

The directional coupler which has compact γ type structure is shown in Fig.1. It is made of two identical dielectric waveguides, coupled each other by sidewall. There is no gap between two guides, so they can be tied up together with binder to get good repeatability and mechanistic stability. The coupling factor K_c is

$$K_c = (\beta_1 - \beta_2)/2 \quad (1)$$

where β_1, β_2 are the propagation constants of symmetrical and antisymmetrical mode respectively, or, the fundamental and second mode if we regard the two waveguides as one.

The coupling length of 3dB coupler is:

$$L_{3dB} = \pi/K_c \quad (2)$$

Because of large aspect ratio of the guides, the effective dielectric constant approach can be used for enough accuracy.

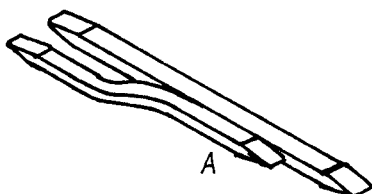
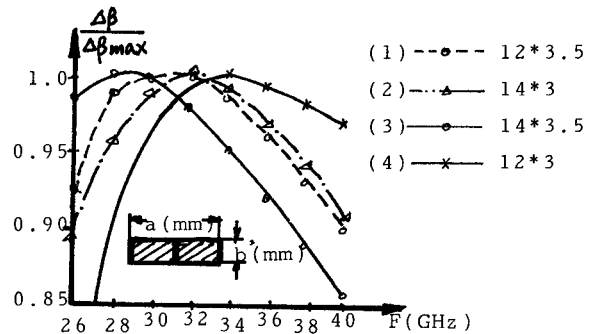


Fig.1 Directional Coupler

We can make the frequency response of coupler flatter by methods as described following:

- 1) Select optimal structure parameters of coupler such as dielectric constant ϵ_r , or cross section of waveguides. The strong coupling where the gap between waveguides is zero can offer broadband

performance, because it's coupling doesn't depend on evanescence field. In strong coupling, if we select proper cross section, we can get flatter frequency response. In Fig.2 are shown several calculated curves of different cross section, their dielectric constant ϵ_r is 2.5 (Polystyrene). Among these curves, curve (1) is a satisfied one.

Fig.2 Normalized coupling factor K_c 2). Take γ type structure.

The part A in Fig.1 is a port of coupling waveguide, which takes the shape of taper in E-plane. It acts as a matched load. So we can save a connecting arm which usually makes frequency response worse.

3). Taper in E-plane.

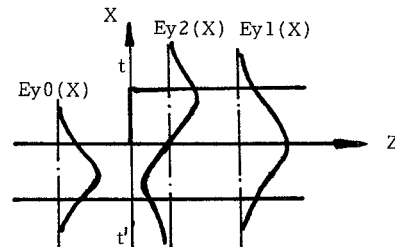


Fig.3 The modes of a coupler

When input wave comes to the taper A, the fundamental mode in single waveguide becomes symmetrical and antisymmetrical mode in coupled waveguides as shown in Fig.3. The abrupt change of shape in $t-t'$ plane can stimulate enough antisymmetrical mode to get correct coupling. The numerical analysis can be carried on by mode matching technique. The taper in E-plane can

reduce the reflection to a level that can be neglected.

The measurement performance of 3dB coupler is shown in Fig.4. The cross section and coupling length of this coupler is same as curve (1) in Fig.2. In the frequency range from 28 to 38 GHz, the coupling unflatness is less than 1dB. The loss of launching, mode transforming and loss of dielectric waveguide is about 1dB.

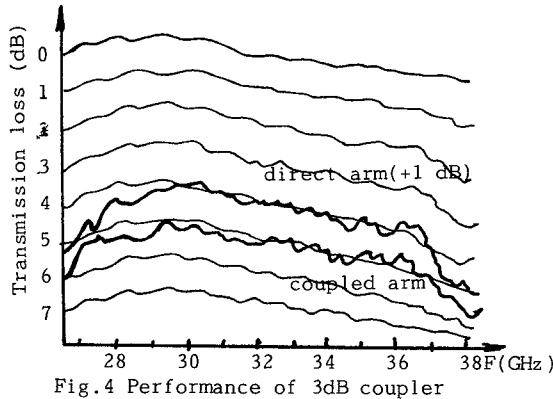


Fig.4 Performance of 3dB coupler

The coupling coefficient of a coupler can be changed by changing its coupling length, not necessary to change its cross section, so the frequency response can be kept unchanged almost. In Fig.5 is shown the performance of 6dB coupler.

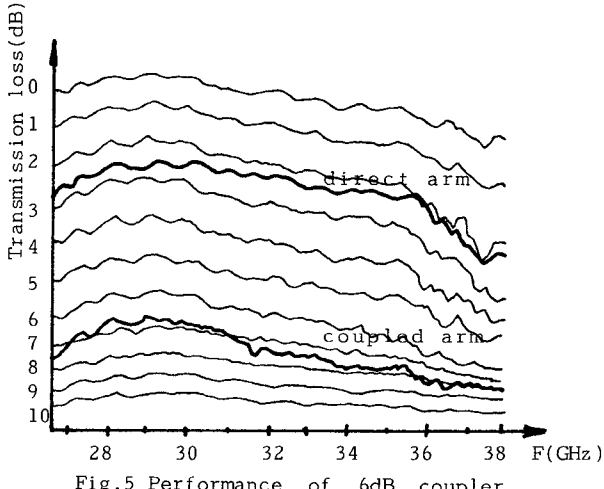


Fig.5 Performance of 6dB coupler

When coupler is used in 6-port network, the phase relationship of two output arms is very important.

If we take assuming that field distribution is sine-shaped in the dielectric and exponential-shaped in the air as shown in Fig.6, the phase relation can be formulated as following:

The field on coupling area can be expressed as:

$$E_y(x, z) = C_1 E_{y1}(x) \exp(j\beta_1 z) + C_2 E_{y2}(x) \exp(j\beta_2 z) \quad (3)$$

where z is the distance from $t-t'$ plane, C_1, C_2 are

mode's amplitudes. So the phase of each point in x, z plane is (when z fixed, $z=z_0$):

$$\varphi(x, z_0) = \tan^{-1} \left(\frac{C_2 E_{y2}(x) \sin(\beta_1 - \beta_2) z_0}{C_1 E_{y1}(x) \cos(\beta_1 - \beta_2) z_0 + C_2 E_{y2}(x)} \right) - \beta_1 z_0 \quad (4)$$

When coupling is weak, we assume that

$$C_1 \approx C_2, |E_{y1}(x)| \approx |E_{y2}(x)|$$

so that,

$$\varphi(x, z_0) = \tan^{-1} \left(1 / (\text{ctan}(\beta_1 - \beta_2) * z_0 \pm 1) \right) - \beta_1 z_0 \quad (5)$$

The phase distribution vs. distance from center of coupling waveguides is shown in Fig.7.

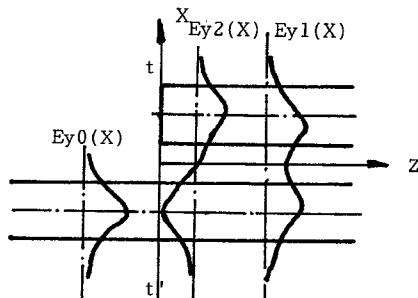


Fig.6 Field distribution on the coupler

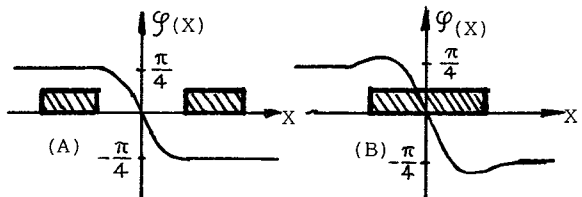


Fig.7 The phase distribution of coupling waveguides
(A) Weakly coupling
(B) Strong coupling

The phase difference between two output arms is (weak coupling):

$$\Delta\varphi = \tan^{-1} \left(\frac{\sin((\beta_1 - \beta_2)l)}{\cos((\beta_1 - \beta_2)l) + 1} \right) - \tan^{-1} \left(\frac{\sin((\beta_1 - \beta_2)l)}{\cos((\beta_1 - \beta_2)l) - 1} \right) = \pi/2 \quad (6)$$

In strong coupling case, the phase difference is approximate 90° , which is identified by measurement as shown in Fig.8.

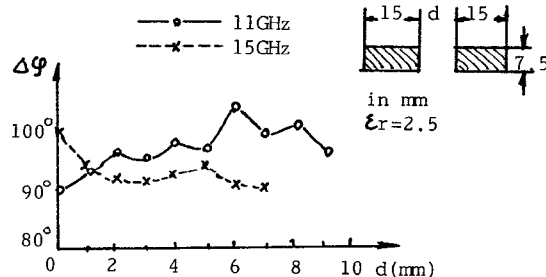


Fig.8 Phase difference between two output arms vs. distance d

Power Divider

Compact Y type power divider is sketched in Fig.9. It is composed of three identical rectangular dielectric waveguides. Both gaps between them are zero, so we can regard the three coupling guides as one.

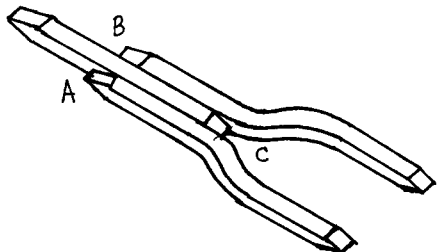


Fig.9 Power Divider

The field on the coupling area can be decomposed into fundamental and third mode, the transverse distribution of them are shown in Fig.10.

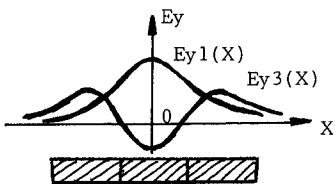


Fig.10 Fundamental and third mode of coupling dielectric waveguides

The field in coupling area is:

$$Ey(x, z) = C_1 E_{yl}(x) \exp(j\beta_1 z) + C_3 E_{y3}(x) \exp(j\beta_3 z) \quad (7)$$

The sketch of measured field distribution of power divider is shown in Fig.11. If we properly select the coupling length, we can get the desired coupling.

The coupling factor K_d is:

$$K_d = (\beta_1 - \beta_3)/2 \quad (8)$$

where β_1, β_3 are the fundamental and third mode's propagation constants, which can be calculated by effective dielectric constant method. Some results are shown in Fig.12.

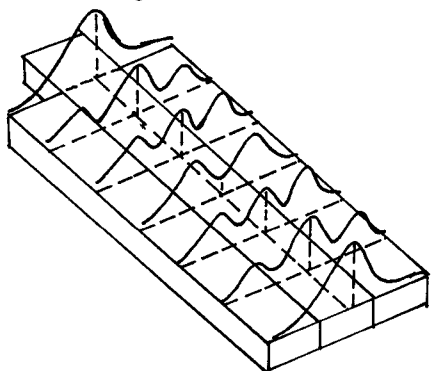


Fig.11 Distribution of $Ey(X, Z)$ of power divider

For the similar reasons as in the case of coupler, this structure is also a broadband one. If

we let power divider as the structure as in Fig.9, where tapers A,B,C act as matched loads, we can make the frequency response flatter.

The coupling length of divider, different from coupler, is:

$$L_{3dB} = 2\pi/K_d \quad (9)$$

In this length the loss of divider is minimum.

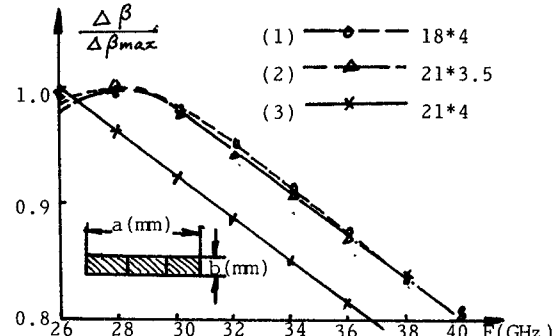


Fig.12 Normalized coupling factor K_d

Six-port Network

The circuit of six-port network is shown in Fig.13, the prototype of which is recommended by Engen (4). The dielectric material is polystyrene, the cross section is $3.5 \times 6 \text{ mm}^2$. The launchers are metal rectangular horns, the ends of waveguide are tapered, and inserted into the horn. Because of strong coupling, the length of coupler becomes shorter, so the size of six-port network becomes smaller, all of the devices can be linked up together and put in a box of size $180 \times 300 \times 30 \text{ mm}^3$, supported by foam polystyrene.

The Q-point of six-port network is depended on coupling of each coupler and power divider, because it is very easy to change the coupling coefficient, namely, only changing the coupling length of the coupler, we can adjust them to proper values, and get desired Q-point distribution easily.

The measured data of Q-point are shown in Table 1.

Acknowledgment

The author would like to thank Mrs. Wang Jia-zhang, Li Li and Wu Jian-xiang for their offering of measurement data and helpful discussions. The author also wishes to thank Prof. Gao Bao-xin and Prof. Zhang Xue-xia for their good suggestions and encouragements.

References

- (1) E.A.J. Marcatilli, "Dielectric Rectangular Waveguide and Directional Coupler for Integrated Optics", BSTJ, Vol. 48, 1969
- (2) D. Radovish, "Coupler for 94 GHz Network Analyzer", Microwave Journal, 1982, pp 90-97
- (3) J.A. Paul and P.C.H. Yen, "Millimeter-wave Passive Components and Six-Port Network Analyzer in Dielectric Waveguide", IEEE-MTT 29, No. 9, 1981

(4) G.F.Engen, "The Six-Port Reflectometer:
An Alternative Network Analyzer"
IEEE MTT-25, No.12, 1977

| Freq. (GHz) | Q1 | Q2 | Q3 | Q4 |
|-------------|-----------------------|-----------------------|-----------------------|----------------------|
| 31 | $3.95\angle-37^\circ$ | $4.43\angle120^\circ$ | $3.23\angle204^\circ$ | $114\angle157^\circ$ |
| 32 | $2.99\angle90^\circ$ | $2.69\angle225^\circ$ | $1.90\angle-63^\circ$ | $12\angle226^\circ$ |
| 33 | $2.04\angle190^\circ$ | $3.44\angle-33^\circ$ | $2.72\angle54^\circ$ | $15\angle210^\circ$ |
| 34 | $2.31\angle-15^\circ$ | $3.18\angle132^\circ$ | $2.30\angle199^\circ$ | $53\angle54^\circ$ |
| 35 | $2.02\angle85^\circ$ | $2.79\angle227^\circ$ | $2.10\angle270^\circ$ | $16\angle243^\circ$ |
| 36 | $1.62\angle220^\circ$ | $2.61\angle14^\circ$ | $2.65\angle64^\circ$ | $6.2\angle18^\circ$ |

Table 1 Q-point of Six-Port Network

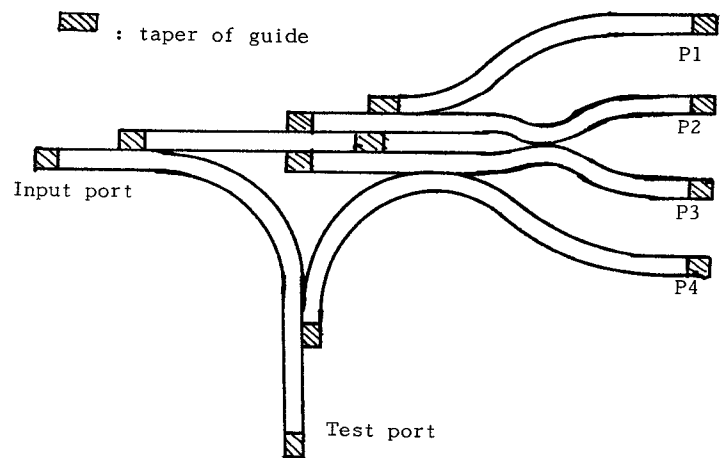


Fig.13 The six-port network